IJBBE International Journal of Biophotonics & Biomedical Engineering Vol. 3, No. 2, Summer-Fall, 2023

Research Article

Reduced Biofilm Formation of *Pseudomonas Aeruginosa* by Silver-Modified Iron Oxide

D. Kabudanian Ardestani [a], R. Safaeijavan *[, b], S. Zare-Karizi [a]

a Department of Biology, Varamin-Pishva Branch, Islamic Azad University, Varamin, Iran
b Department of Biochemistry and Biophysics, Varamin-Pishva Branch, Islamic Azad University, Varamin, Iran

***Corresponding author: safaeijavan@gmail.com**

DOI: 10.30495/ijbbe.2024.2004867.1039

ABSTRACT

Received: Dec. 31, 2023, Revised: Jan. 23, 2024, Accepted: Jan. 2, 2024, Available Online: Feb. 5, 2024

Objectives and Background: *Pseudomonas aeruginosa (P. aeruginosa) is a nosocomial opportunistic pathogen. Considering the importance of biofilm in the pathogenicity and resistance of these bacteria, efforts should be made to find new antibacterial compounds.*

Methods: *The Fe_3O_4 nanoparticles were synthesized by the co-precipitation method and were modified by the $AgNO_3$ reductive solution to investigate the influence of Ag-Fe_3O_4 nanoparticles on the biofilm formation of P. aeruginosa. The synthesized nanoparticles' properties were determined by FESEM, DLS, FTIR, XRD, and Zeta potential tests.*

Results: *FESEM and DLS revealed a cubic and smooth structure with an average size of 44.36 nm. XRD analyses confirmed the presence of a magnetite core. FTIR spectrum determined the existence of silver plating on the magnetic surface. The Zeta potential results indicated that the magnetic nanoparticles' surface net charge was 24.4 and the surface net charge for silver-modified nanoparticles was -28.3. Finally, after separating 40 isolates of P. aeruginosa among 82 clinical isolates as strong biofilm producers, then the inhibitory effect of synthesized Ag- Fe_3O_4 nanoparticles on the formation of biofilms was studied using the broth micro-dilution method.*

Conclusions: *Accordingly, it was proved that Ag-Fe_3O_4 nanoparticles can be used to treat biofilm infections and were introduced as the new antimicrobial agents.*

KEYWORDS

Ag-Fe_3O_4 nanoparticles; Biofilm; Composite; Iron oxide nanoparticles; P. aeruginosa.

I. INTRODUCTION

Over the past decades, magnetic iron oxide nanoparticles have been of great interest to researchers due to their very valuable potential applications in various fields including Ferro-fluids, catalysts, and high-density magnetic recording media [1]. Magnetite iron oxide nanoparticles are one of the most important and acceptable nanoparticles for medical applications [2].

Iron oxide is found in various forms in nature. The most common are Magnetite (Fe_3O_4), Magnetite (γ-Fe_2O_3), and Hematite (α-Fe_2O_3). Magnetite is a common magnetic iron oxide that has a cubic inverse spinel structure [3].

The preparation of magnetite iron oxide nanoparticles in a very narrow size range that displays the super-paramagnetic properties is of special attention [4]. Iron-oxide nanoparticles could generate oxidative stress by ROS including superoxide radicals, hydroxyl radicals, hydrogen peroxide, and singlet oxygen which may cause chemical damage to proteins and DNA in bacteria. According to published studies, these nanoparticles could reduce biofilm formation effectively [5]

The selection of the preparation method for magnetic nanoparticles is dependent on further usage. For example, the magnetic carriers in nanotechnology and the medical profession require a defined composition and size, and excellent stability in aqueous conditions in organic as well as aqueous solvents in a wide range of pH [6]. Thus, several pathways for the preparation of Fe_3O_4 nanoparticles have been published in other papers, such as biological synthesis [7,8], energy milling [9], reducing [10], and ultrasonic-assisted impregnation [11]. The co-precipitation method is one of the best methods of synthesis due to its simplicity, cheapness, and reproducibility [12, 13].

After synthesis, Fe_3o_4 nanoparticles need surface modification to make them more adequate for bio-systems. Iron oxide nanoparticles coated with a thin layer of Au or Ag, are a well-known composite system that enhances the optical and magnetic properties compared to their single-component materials. So, many works report on the preparation and properties of noble metal/Fe_3O_4 core-shell nanoparticles [14].

By introducing a positive charge to the surface of nanoparticles when such coatings are applied, the interplay between the negative charges on the cell membrane will increase the nanoparticles captured and can lead to easy cellular uptake [15, 16].

Silver is a well-known substance that has been used for centuries as an antibacterial agent [17]. Silver has also gained a lot of attention due to the increased risk of antibiotic resistance, which is the result of the indiscriminate use of antibiotics [18].

The emersion of new strains of antibiotic-resistant bacteria has become a serious issue in public healthcare. Therefore, there is a strong motivation to develop new bactericides. Silver has an important advantage over antibiotics as it kills all pathogenic microorganisms, and no organism has ever been reported to resist it [6]. In addition, the binding of magnetic nanoparticles with silver can preserve the optical and magnetic properties of the relevant components [19].

P. aeruginosa is a gram-negative bacterium found in water, soil, plants, and humid environments in hospitals. These bacteria are a major cause of nosocomial lung infections and a source of wound infections, especially in thermal burns [20-22]. *P. aeruginosa* has been identified as an opportunistic pathogen. The importance of *P. aeruginosa* is mainly related to its high resistance against antibacterial drugs and to its inherent resistance to antibiotics, which becomes resistant to the drugs during the treatment [23]. Survival and virulence of this bacterium are related to the biofilms it produces. Biofilms are sessile communities that form on both biotic and abiotic surfaces [24]. An important factor in the stability and resistance of *P. aeruginosa* biofilms is the extracellular polymeric substance (EPS), which supplies the scaffolding to maintain the colony.

The EPS is a complex matrix composed of various macromolecules and forms a dense structure against antibiotics [24, 25].

In this paper, we used a simple route for the synthesis of dispersed core-shell nanostructures of Ag-Fe_3O_4. Also, the antibacterial activity of the composite magnetic nanoparticles was tested on the biofilm of *P. aeruginosa*.

II. Materials and Methods

A. *Materials*

Ferric chloride [$FeCl_3$], ferrous chloride [$FeCl_2$], ammonia [NH_3], crystal violet, and sodium hydroxide [NaOH] were purchased from Merck, Germany. All the reagents used for the synthesis of Fe_3O_4 were analytical grade and were obtained from Merck.

B. *Bacterial strains and culture media*

82 clinical isolates of *P. aeruginosa* strains from Taleghani Hospital were used in this study. Muller Hinton (MH) agar, Tryptic soy broth (TSB), tryptic soy agar (TSA), Eosin Methylene Blue (EMB), Triple Sugar Iron (TSI) Agar, 82 clinical isolates of *P. aeruginosa* strains from Taleghani hospital were used in this study. Muller Hinton (MH) agar, Tryptic soy broth (TSB), tryptic soy agar (TSA), Eosin Methylene Blue (EMB), Triple Sugar Iron (TSI) Agar and Simmons Citrate Agar were purchased from Merck Company and used as culture media.

C. *Identification of P. aeruginosa*

In this study, 82 *Pseudomonas* strains originated from clinical samples (wound, urine, phlegm, body fluid, and blood) of hospitalized patients from the Taleghani Hospital, Tehran, Iran during June-July, 2017. The isolates were identified and confirmed by microbiological and biochemical tests that included oxidase, catalase, sulfide indole motility (SIM), triple sugar iron (TSI) agar, oxidation fermentation (OF) test, growth at 42˚C, Methyl Red Voges Proskauer (MR-VP), as well as pyocyanin production in Mueller Hinton agar.

D. *Synthesize of Fe_3O_4 nanoparticles*

Iron oxide nanoparticles were obtained by the precipitation method [26]. 2.307 g ferric chloride 6 hydrate ($FeCl_3 \cdot 6H_2O$), and 3.97 g ferrous chloride 4 hydrate ($FeCl_2.4H_2O$) were dissolved in 100 mL of deoxygenated deionized water. The mixed solution was heated at 85 °C for 30 minutes. A volume of 7.47 ml NH_3 was adjusted to 100 ml and was added dropwise to the solution. After 2 hours of stirring, the mixtures were cooled down to room temperature, and the magnetic Fe_3O_4 nanoparticles were separated by the external magnetic field. The particles were rinsed with ethanol and distilled water and dried at 40°C [27]. The related chemical reaction can be expressed as follows equation 1:

$$Fe^{2+} + 2Fe^{3+} + 8OH^- \rightarrow Fe_3O_4 + 4H_2O \quad (1)$$

E. *Surface modification*

0.67 g of $AgNO_3$ was mixed with 100 ml ethanol. Also, Silver nitrate concentration was fixed to get mass ratio Ag: Fe_3O_4 = 1:100 and added to the $AgNO_3$ solution. The mixture of Fe_3O_4 nanoparticles and silver nitrate was sonicated for 15 min. The polypropylene container was applied to avoid non-specific silvering of the reaction dish. Next, the ethanol solution of 19% butyl-amine (as a weak reductant agent) was dropwise added to the mixture, and the whole of the reagents was sonicated at 50 °C for 45 minutes. The nanoparticles were separated by the external magnetic field and were rinsed with alcohol and distilled water. Finally, Ag-Fe_3O_4 composite magnetic nanoparticles dried at 45 °C for 2 hours in the oven.

F. *Charactrization of Fe_3O_4 and Ag-Fe_3O_4 nanoparticles*

The structural investigation of Fe_3O_4 and Ag-Fe_3O_4 was studied by recording their powder X-ray Diffraction (XRD) patterns. A copper anode emitting Cu Kα radiation (Panalytical X'Pert PRO, Netherlands) was applied to record patterns. The morphology of the materials was examined by Scanning Electron Microscopy (ZEISS SIGMA VP SEM, Germany). Dynamic

light scattering (DLS) and the zeta potential measurements were done by a Malvern Zeta size analyzer instrument (Malvern3600 Instruments Ltd., Malvern, UK) to investigate the size distribution pattern and average particle size of the synthesized crystallites. The zeta potential measurements were applied in samples prepared with distilled water and after vigorous stirring. The functional groups present on the surface of Fe_3O_4 and Ag-Fe_3O_4 particles were defined by Fourier transform infrared spectroscopy (FTIR) using Thermo Scientific Nicolet 380 equipment.

G. *The ability of isolates for biofilm formation*

Determination of biofilm formation was carried out for all 82 isolates by the microtiter plate method. Cultures were inoculated in TSB and adjusted to 0.5 McFarland standards. Every three wells of a 96-well plate were filled with 100 µL of bacterial suspension. The negative control contained just TSB. Then, plates were incubated for 24 hours at 37°C. Afterward, the content of each well was rinsed two times with 200 µL of sterile Phosphate buffered saline (PBS), emptied, and left to dry. Then, the plates were stained for 10 minutes with crystal violet. The excess stain was rinsed with water and air-dried. In the last step, the wells were filled with 100 µL of 33% (v/v) glacial acetic acid. The optical density (OD) of stained biofilms was studied by using a micro ELISA auto reader (model 680, Biorad, UK) at wavelength 570 nm. All tests were repeated three times and the final data was then averaged. The description of biofilm formation was done according to the criteria of Stepanovic et. al. as shown in (Table 1) [28-30].

Table **1** Interpretation of biofilm production. Optical density cut-off value (ODc) = average OD of negative control + 3x standard deviation (SD) of negative control

Average OD value	Biofilm production
≤ ODc / ODc < ~ ≤ 2x ODc	Non / Weak
2x ODc < ~ ≤ 4x ODc	Moderate
> 4x ODc	Strong

H. *Determination of minimum inhibitory concentration (MIC)*

The broth micro-dilution method was used to determine the MIC. For this purpose, 100 µl Mueller-Hinton Broth was pipetted into a 96 well-plate, and a stock of suspension of Ag-Fe_3O_4 nanoparticles was prepared at a concentration of 512 µg/ml (5/12 mg of NPs were mixed in 10 ml of Mueller Hinton Broth). Different concentrations (0.25, 0.5, 1, 2, 4, 8, 16, 32, 64, 128, 256 and 512 µg/ml) of nanoparticles were prepared and 100 µg/ml of every concentration mixed with 100 µl of bacterial suspension with turbidity equivalent to 0.5 Mc-Farland. After 24 hours of incubation, 50 µl 2, 3, 5-Triphenyl-tetrazolium chloride solution (TTC) solution (0.5% w/v) was added to each well. The lowest concentration at which color change (red) occurred was considered the lowest concentration of the nanoparticles that inhibited visible bacterial growth. A well-containing medium without nanoparticles and bacterial suspension was used as the medium control. All experiments were carried out two times. All of the above steps were also carried out with Fe_3O_4 nanoparticles before surface coating.

I. *Investigation of biofilm formation ability by strains under the influence of Fe_3O_4 and Ag-Fe_3O_4 nanoparticles*

In the previous step, 40 strains of Pseudomonas that formed a strong biofilm were isolated. The formation of biofilms in isolated strains at different concentrations (8 to 512 µg/ml) of Fe_3O_4 and Ag-Fe_3O_4 nanoparticles was investigated based on the calculation of ODc by micro-titer plate method.

III. Results and Discussion

A. *Investigation of Fe_3O_4 and Ag-Fe_3O_4 nanoparticles*

Scanning microscopy images (Fig.1), show the morphology of iron oxide (Fe_3O_4) and Ag-Fe_3O_4 nanoparticles (Ag-Fe_3O_4). SEM images showed the cubic structure of nanoparticles with a smooth surface and the average size of Fe_3O_4 nanoparticles was about 40 nm. The image of the nanoparticles after surface

modification also shows a cubic structure that has increased in size.

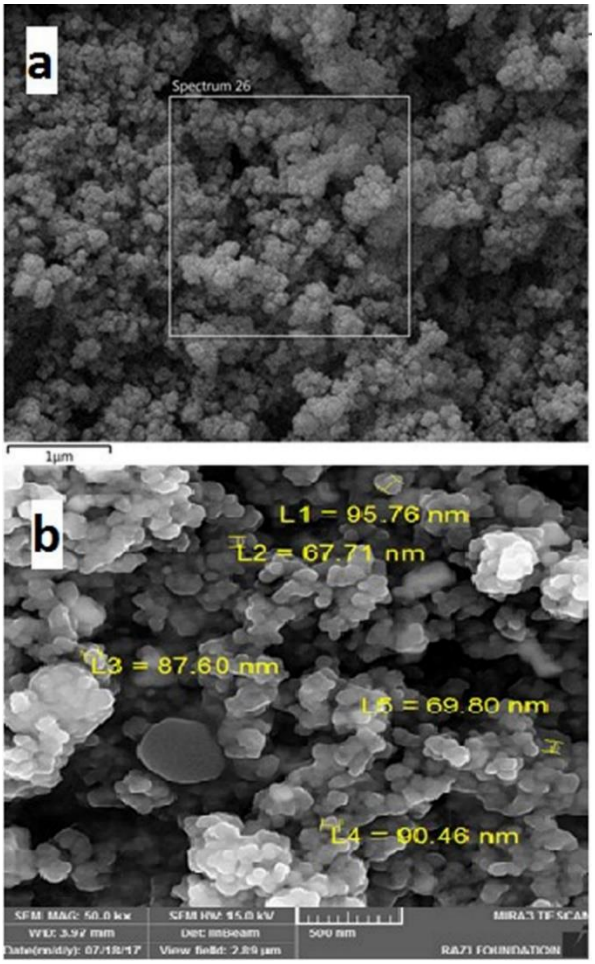

Fig. **1** SEM images of a) Fe_3O_4 particles and b) Ag-Fe_3O_4 composite particles.

The EDS spectra of synthesized Fe_3O_4 (Fig. 2) indicated the obvious peaks of Fe and O and revealed that it is composed of Fe (83.2%) and O (16.8%) elements. The results showed the purity of the synthesis Fe_3O_4.

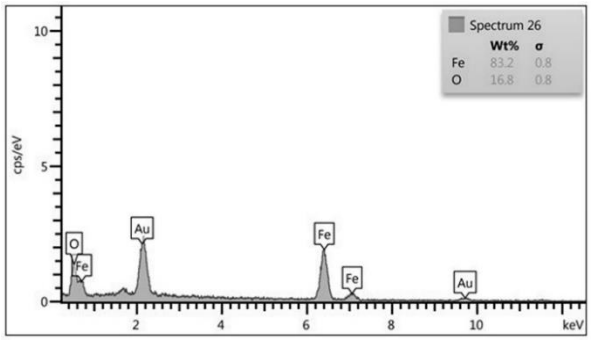

Fig. **2** EDS image of Fe_3O_4.

Accurate information about the size distribution of Fe_3O_4 and Ag-Fe_3O_4 was received from the DLS measurements. The Fe_3O_4 particles had an average size of 39.75 nm and the peaks with maxima at approximately 44.36 nm size were reported for Ag-Fe_3O_4 nanoparticles (Fig. 3). Unsoy et. al. in 2012, reported mean diameters of iron oxide nanoparticles 18 nm. Since nanoparticles with a size below 100 nm can penetrate cells, these particles are acceptable [31].

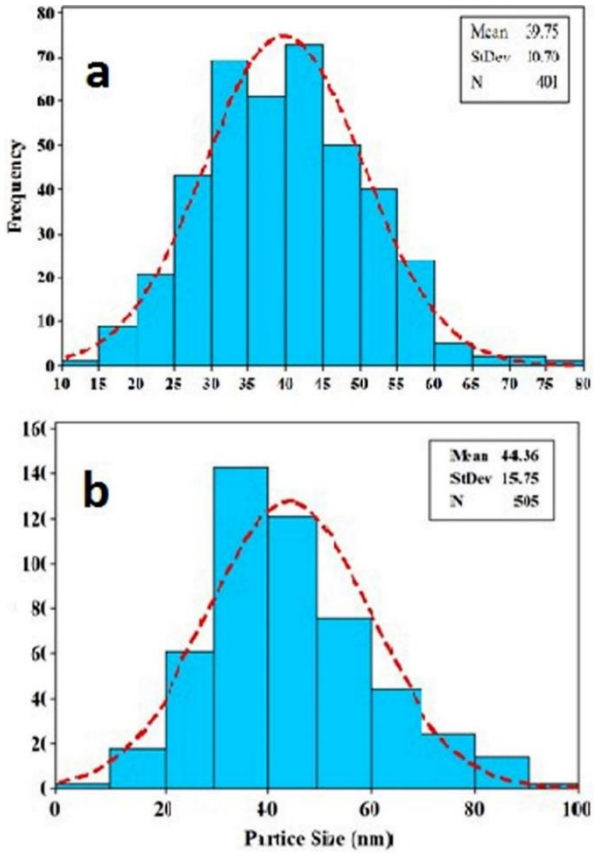

Fig. **3** DLS spectrum of size distribution observed for a) Fe_3O_4 and b) Ag-Fe_3O_4 nanoparticles.

(Figure 4) shows typical powder XRD patterns of Fe_3O_4 and Ag-Fe_3O_4 composite particles. The experimentally obtained patterns were identified through comparison with standard Fe_3O_4 and Ag patterns (PDF standard cards). The X-ray diffraction pattern of obtained magnetite shows reflection planes (220), (311), (222), (400), (422), (511), and (440) which can be indexed as planes of Fe_3O_4 (PDF, no. 19-0629). This indicated that the synthesized nanoparticles were pure Fe_3O_4. After Ag

coating, four additional peaks were observed at 38.28, 44.4, 64.59, and 77.51, corresponding to (111), (200), (220), and (311) planes of silver, respectively, with cubic structure. Bani Asadi et al. in 2014, also synthesized iron oxide nanoparticles. As a result of the XRD test from this study, the space between the d-value plates with the values between the crystallographic plates extracted from the data of the standard issue code 19-0629 of the standard panel discriminant committee is close to that of Fe_3O_4 as confirmed by the present study [32].

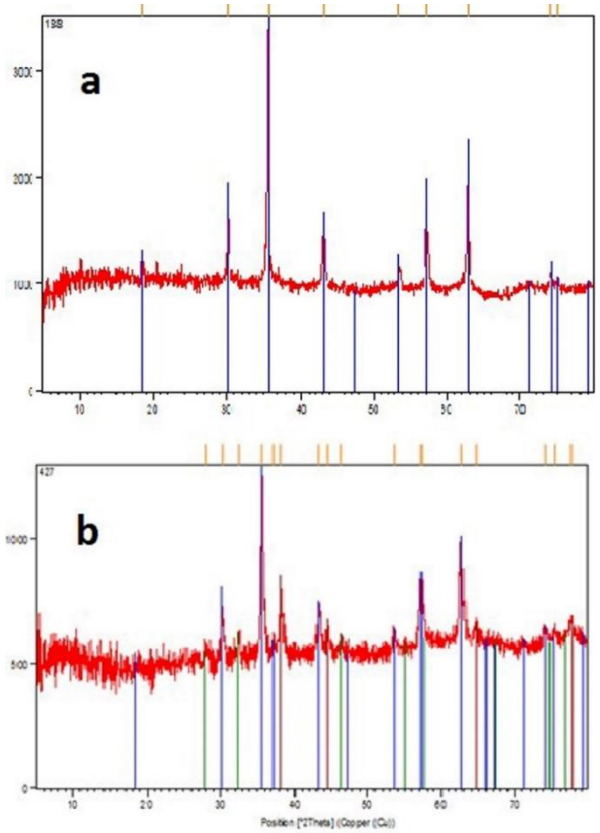

Fig. **4** XRD spectra of a) Fe_3O_4 nanoparticles and b) Ag-Fe_3O_4 core-shell nanoparticles.

The Zeta potential curve (Fig. 5) for the synthesized Fe_3O_4 nanoparticles indicated that the pure surface charge of Fe_3O_4 is 24.4. The charge of the nanoparticles after the surface modification was also measured and the zeta potential of -28.3 was recorded for these particles. This result shows that the colloidal solution of silver-modified iron nanoparticles is well-established.

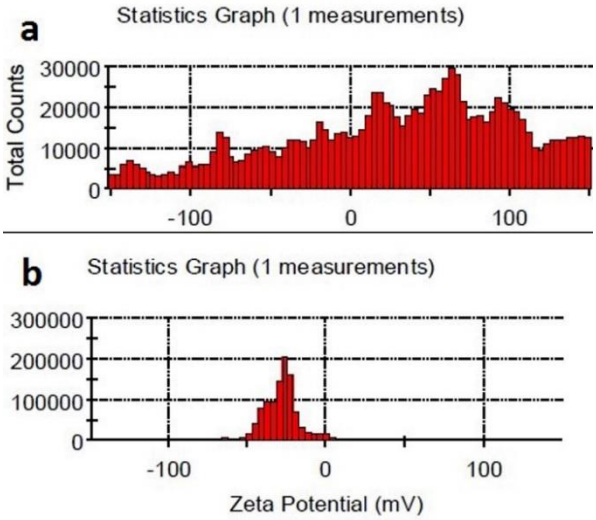

Fig.**5** The zeta potential of a) Fe_3O_4 and b) Ag-Fe_3O_4 nanoparticles.

FTIR studies (Fig. 6) showed the presence of a powerful absorption line in both coated and pure Fe_3O_4 located at 579 cm^{-1} that was attributed to the stretching vibration of

Fe-O in tetrahedral sites. The peaks at 1618-3415 cm^{-1} are assigned to the bending of the O-H stretching vibration. The absorption peak at 1271 cm^{-1} is assigned to the bending of N–H and C–N of butyl-amine which indicates there are some butyl amine residues present in the core-shell nanoparticles. In the research of Hasanzadeh et al in 2014, in the graphs of the FTIR spectrum of the iron oxide nanoparticle, the absorption band was observed around the wavelength of 573 cm^{-1} in the uncoated iron oxide nanoparticles which related to the Fe-O stretching vibration in Fe_3O_4, which is close to the present study and confirms the presence of magnetite nanoparticles [33].

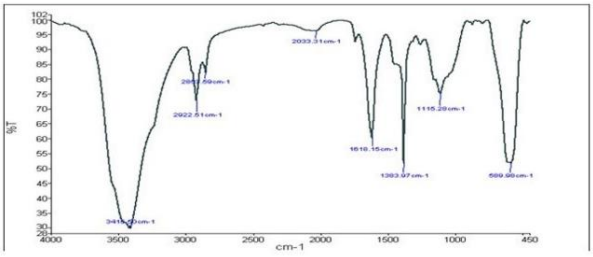

Fig. **6** FTIR spectra of Ag-Fe_3O_4 nanoparticles.

B. *MIC of Fe_3O_4 and Ag-Fe_3O_4 nanoparticles for strong biofilm producer's P. aeruginosa*

According to the micro-titer plate results, among 82 isolates of *P. aeruginosa*, 40 isolates were detected as strong biofilm producers and selected for further experiments. Mohammadi Mehr et al. in 2004, examined 42 clinical specimens of *P. aeruginosa* using micro-titer plate and electron microscope images. This study considered the micro-titer plate method easier and more economical for diagnostic use [34].

MIC of Fe_3O_4 and Ag-Fe_3O_4 were determined for these 40 isolates of strong biofilm producers *P. aeruginosa.* The MIC results indicated that the Fe_3O_4 nanoparticles showed minimum inhibition against 6 isolates (15%) at the concentration of (256 µg/ml), 14 isolates (35%) at the concentration of (512 µg/ml), and 20 isolates (50%) at the concentration of (>512 µg/ml). Also, the MIC results illustrated that the MIC of the modified Fe_3O_4 nanoparticles were as follows: 1 isolate (2.5%) =8 µg/ml, 1 isolate (2.5%) =16 µg/ml, 3 isolates (7.5%) =32 µg/ml, 3 isolates (7.5%) =64 µg/ml, 10 isolates (25%) =128 µg/ml, 10 isolates (25%) =256 µg/ml, 9 isolates (22.5%) =512 µg/ml and 3 isolates (7.5%) more than 512 µg/ml which represents the stronger anti-biofilm effect of silver modified iron oxide nanoparticles than uncoated Fe_3O_4.

(Fig. 7) shows the results of the relative frequency of strong *p. aeruginosa* strains MIC under the influence of iron oxide nanoparticles and Ag-Fe_3O_4 nanoparticles. The MIC of strong biofilm producer *P. aeruginosa* affected by iron oxide nanoparticles was a very high concentration of these nanoparticles (256 µg /mL) in 15% of the strains studied. While the MIC of silver-modified nanoparticles was obtained at a very low concentration so that 2.5% of the strains at a concentration of (8 µg/mL), the lowest concentration of the study, inhibited biofilm growth.

45% of the strains in the concentration below (256 µg/mL), the first concentration in the unmodified nanoparticles affected bacterial biofilms, have inhibited the growth of the biofilm of this bacterium. In other words, silver-modified nanoparticles have the effect of inhibiting the growth of bacterial biofilms at lower concentrations. The graph shows that the growth of 50% of the strains studied was affected by the highest concentration of iron oxide nanoparticles, while only 7.5% of the strains treated with silver-modified nanoparticles required such a high concentration to inhibit biofilm growth. These results showed the stronger anti-bacterial effect of Ag-Fe_3O_4 nanoparticles than uncoated Fe_3O_4 on *P. aeruginosa* biofilms. Nangmenyi et al. in 2011, used silver-modified iron nanoparticles to control water contamination. The results of this study also proved that the presence of silver and iron simultaneously increases their antimicrobial properties [35].

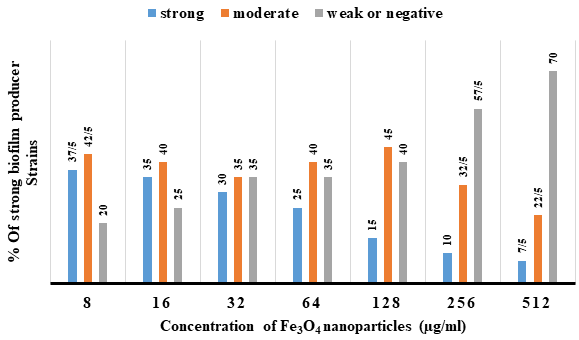

Fig.**7** The results of the relative frequency of strong p. aeruginosa strains MIC under the influence of iron oxide and Ag-Fe_3O_4 nanoparticles.

C. *Biofilm formation of P. aeruginosa strains under the influence of Fe_3O_4 and Ag-Fe_3O_4 nanoparticles*

The results of the biofilm formation study in 40 isolated strong producer biofilm strains of *P. aeruginosa* under the influence of iron oxide nanoparticles and silver-modified iron oxide nanoparticles are summarized in (Fig. 8).

As can be seen, the inhibition of biofilm formation in different strains has been affected by different nanoparticles; in fact, the degree of resistance of each clinical strain to treatment is different. Also, silver-modified iron

nanoparticles had a much stronger effect in inhibiting biofilm formation, so that at the lowest concentration of Fe_3O_4 nanoparticles, 37.5% of the strains still form strong biofilms, while at this concentration of Ag-Fe_3O_4 nanoparticles, the amount of strong biofilm is reduced to 25%. With increasing the concentration of nanoparticles in both groups, a decrease in strong biofilm formation and an increase in inhibition of biofilm formation is observed. Finally, even at the highest concentrations of iron nanoparticles, 7.5% of the strains formed a strong biofilm, whereas due to the concentration of 32µg/ml of Ag-Fe_3O_4 nanoparticles, this amount of strong biofilm was formed, and at a concentration of 512µg/ml, in all the strains were inhibited. The results of this study showed that if modified silver-coated iron oxide nanoparticles are used, lower concentrations of these nanoparticles are required to inhibit the formation of bacterial biofilm.

Studies to date have shown that the effect of nanoparticles on bacterial biofilms depends on a variety of factors, including biofilm properties, biofilm mass volume, pore size, number and type of bacteria, and electric charge of the biofilm as a biopolymer. Also mentioned are nanoparticle properties such as nanoparticle type, particle size distribution, and particle surface electric charge. Therefore, in investigating how nanoparticles affect bacterial biofilms, we are faced with various factors. Since the pore diameter of the biofilm is reported to be about 50 nm, particles of this size or smaller are expected to have better permeability and thus greater toxicity.

Since the surface charge of the biofilm mass is reported to be negative in most cases, positively charged particles due to electrostatic attractions are likely to have a better ability to penetrate bacterial biofilms. The role of proteins that bind to nanoparticles is also important in creating toxicity and antibacterial properties. In 2016, Javanbakht et al. examined two types of magnetic iron particles modified with the amine group for positive charge and the carboxyl group for negative charge. Their studies showed that the toxicity of positively charged nanoparticles was higher than that of neutral nanoparticles and the toxicity generated by neutral nanoparticles was higher than that of negatively charged nanoparticles. They argued that the result was better absorption of positively charged particles into the bacterial biofilm and less absorption of negatively charged nanoparticles due to electrostatic repulsions [36].

Since in the present study the positive charge is related to iron oxide nanoparticles and the negative charge is related to silver-modified iron oxide nanoparticles and the mechanism of the effect of iron and silver on bacterial biofilms is different, it becomes more difficult to discuss this. Iron oxide nanoparticles are more bound to the surface of the biofilm and less penetrate the biofilm. Negative charging of exopolysaccharides prevents the binding of silver-modified nanoparticles to the negatively charged surface of the biofilm and increases the penetration of silver-modified nanoparticles into the biofilm. A high surface-to-volume ratio releases more silver ions and produces activated oxygen, killing the biofilm of the bacterium.

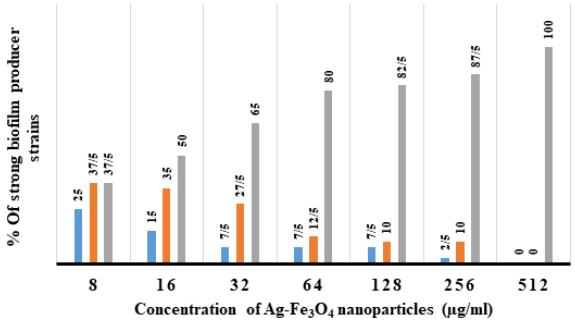

Fig.**8** The results of the relative frequency of strong p. aeruginosa strains biofilm formation under the influence of different concentrations of Fe_3O_4 and Ag-Fe_3O_4 nanoparticles.

IV. Conclusion

One of the most important pathogenic species that can produce biofilms is *P. aeruginosa*. A biofilm is a structured consortium of bacteria embedded in a polymer matrix consisting of polysaccharides, proteins, and DNA. Bacterial biofilms cause chronic infections because they show increased tolerance to antibiotics and disinfectant chemicals as well as resisting

phagocytosis and other components of the body's defense system. *P. aeruginosa* is an opportunistic gram-negative bacterium that is found in water and soil and can survive with low levels of nutrients and grow in temperatures ranging from 4-42°C. These characteristics allow it to attach itself and survive on medical equipment and other hospital surfaces. Infections due to P. aeruginosa are difficult to eradicate because of their elevated intrinsic resistance as well as their capacity to acquire resistance to different antibiotics [33, 34]. In conclusion, a simple method of the preparation of magnetic Fe_3O_4 nanoparticles was used. Fe_3O_4 nanoparticles were synthesized by a chemical co-precipitation route with a size of 40 nm. Afterward, the obtained nanoparticles were coated with Ag. The results showed that Ag-Fe_3O_4 nanostructures could inhibit the biofilm formation of *P. aeruginosa* at examined concentrations in this study. Also, the results showed a stronger anti-bacterial effect of Ag-Fe_3O_4 nanoparticles than uncoated Fe_3O_4 on *P. aeruginosa*. Also, this study showed that under the influence of Ag-Fe_3O_4 nanoparticles, strong biofilms of *P. aeruginosa*, were either destroyed or converted to weaker levels which means that, Ag-Fe_3O_4 nanoparticles can be used to treat biofilm infections and were introduced as the new antimicrobial agents.

ACKNOWLEDGMENT

The authors are thankful to the Varamin Pishva branch, Islamic Azad University for providing the materials and laboratory equipment for this study.

FUNDING

This study was part of the student thesis of the biological sciences faculty, Varamin Pishva branch, Islamic Azad University.

CONFLICT OF INTEREST

The authors declare that they have no conflict of interest.

REFERENCES

[1] K. Kalantari, M.B. Ahmad, K. Shameli, and R. Khandanlou, "Synthesis of talc/Fe_3O_4 magnetic nanocomposites using chemical co-precipitation method," Int. J. Nanomedicine, Vol. 8, pp. 1817 (1-7), 2013.

[2] Q. Pankhurst, N. Thanh, S. Jones, and J. Dobson, "Progress in applications of magnetic nanoparticles in biomedicine," J. Phys. D Appl. Phys. Vol. 42, pp. 224001 (1-15), 2009.

[3] S. Hasany, I. Ahmed, J. Rajan, and A. Rehman, "Systematic review of the preparation techniques of iron oxide magnetic nanoparticles," J. Nanosci. Nanotechnol, Vol.2, PP.148-158, 2012.

[4] A. Pachla, Z. Lendzion-Bieluń, D. Moszyński, A. Markowska-Szczupak, U. Narkiewicz, R.J. Wróbel, and G. Żołnierkiewicz, "Synthesis and antibacterial properties of Fe_3O_4-Ag nanostructures," Pol. J. Chem. Technol. Vol. 18, pp. 110-116, 2016.

[5] M.B. Sathyanarayanan, R. Balachandranath, Y.G. Srinivasulu, S.K. Kannaiyan, and G. Subbiahdoss1, "The Effect of Gold and Iron-Oxide Nanoparticles on Biofilm-Forming Pathogens," ISRN Microbiology, Vol. 2013, pp. 1-5, 2013.

[6] B. Chudasama, A.K. Vala, N. Andhariya, R. Upadhyay, and R. Mehta, "Enhanced antibacterial activity of bifunctional Fe_3O_4-Ag core-shell nanostructures," Nano Res, Vol. 2, pp. 955-965, 2009.

[7] A. Izadi, R. Safaeijavan, E. Moniri, and S.A. Alavi, "Green synthesis of Iron oxide nanoparticles using carum carvi L. and modified with chitosan in order to optimize the anti-cancer drug adsorption." Int. J. Bio-Inorg. Hybrid Nanomater, Vol. 7, pp. 71-78, 2018.

[8] B. Naeimipour, E. Moniri, A. Vaziri Yazdi, R. Safaeijavan and H. Faraji, "Green biosynthesis of magnetic iron oxide nanoparticles using Mentha longifolia for imatinib mesylate delivery," IET Nanobiotechnology, Vol. 16, pp. 225–237, 2022.

[9] B.A. Bolto, "Magnetic particle technology for wastewater treatment," J. Waste Manag. Vol. 10, pp. 11-21, 1990.

[10] A.B. Fuertes and P.A. Tartaj, "facile route for the preparation of superparamagnetic porous

carbons," Chem. Mater. Vol. 18, pp. 1675-1679, 2006.

[11] N. Yang, S. Zhu, D. Zhang and S. Xu," Synthesis and properties of magnetic Fe_3O_4-activated carbon nanocomposite particles for dye removal," Mater. Lett. Vol. 62, pp. 645-647, 2008.

[12] P.L.Hariani, M. Faizal, R. Ridwan and M. Marsi, "Setiabudidaya D. Synthesis and properties of Fe_3O_4 nanoparticles by co-precipitation method to removal procion dye," Int. J. Environ. Sci. Dev. Vol. 4, pp. 336-340, 2013.

[13] S. Azizmohammadi, R. Safaeijavan, A. Heydarinasab ans E. Moniri, "Green Synthesis of Polyvinylpyrrolidone Coated Super-Paramagnetic Fe3O4 Nanoparticles for Controlled Release of Letrozole: A pH-Sensitive Drug Delivery System," J. of Cluster Science, vol. 35, pp. 299-310, 2023.

[14] C. Liu, Z. Zhou, X. Yu, B. Lv, J. Mao, and D. Xiao, "Preparation and characterization of Fe_3O_4/Ag composite magnetic nanoparticles," Inorg. Mater, Vol. 44, pp. 291-295, 2008.

[15] T. Osaka, T. Nakanishi, S. Shanmugam, S. Takahama, H. Zhang, "Effect of surface charge of magnetite nanoparticles on their internalization into breast cancer and umbilical vein endothelial cells," Colloids Surf. B, vol. 71, pp. 325-330, 2009.

[16] M. Mahdavi-Ourtakand, P. Jafari and R. Safaeijavan, "Antibacterial activity of biosynthesized silver nanoparticles from fruit extracts of Bunium persicum Boiss," Int. J. Bio-Inorg. Hybr. Nanomater, Vol. 6, pp. 245-251, 2017.

[17] Z.A. Kalaki, R. Safaeijavan and M.M. Ortakand, "Biosynthesis of Silver Nanoparticles Using Mentha longifolia (L.) Hudson Leaf Extract and Study its Antibacterial Activity," Arch. Biol. Sci. Vol. 8, pp. 24-30, 2017.

[18] Z.A. Kalaki, R. SafaeiJavan and H. Faraji, "Procedure optimisation for green synthesis of silver nanoparticles by Taguchi method," Micro. Nano. Lett. Vol 13, pp. 558-561, 2018.

[19] M.K. Joshi, H.R. Pant, H.J. Kim, J.H. Kim and C.S.Kim , "One-pot synthesis of Ag-iron oxide/reduced graphene oxide nanocomposite via hydrothermal treatment," Colloids Surf. A Physicochem, Vol. 446, pp.102-108, 2014.

[20] J.W. Costerton, P.S. Stewart and E.P. Greenberg, "Bacterial biofilms: a common cause of persistent infections," Science, Vol. 284, pp. 1318-1322, 1999.

[21] M. Radzig, V. Nadtochenko, O. Koksharova, J. Kiwi, V. Lipasova ans I. Khmel, " Antibacterial effects of silver nanoparticles on gram-negative bacteria: influence on the growth and biofilms formation mechanisms of action," Colloids Surf. B, Vol.102, pp. 300-306, 2013.

[22] M. Schaechter, *Encyclopedia of microbiology*, Academic Press 2009.

[23] A. Tsutsui, S. Suzuki, K. Yamane, M. Matsui, T. Konda, E. Marui and Y. Arakawa , "Genotypes and infection sites in an outbreak of multidrug-resistant Pseudomonas aeruginosa," J. Hosp. Infect. Vol. 78, pp. 317-322, 2011.

[24] N. Høiby, T. Bjarnsholt, M. Givskov, S. Molin and O. Ciofu, "Antibiotic resistance of bacterial biofilms," Int. J. Antimicrob Agents, Vol.35,pp. 322-332, 2010.

[25] L. Ma, M. Conover, H. Lu, M.R. Parsek, K. Bayles and D.J. Wozniak, "Assembly and development of the Pseudomonas aeruginosa biofilm matrix," PLOS Pathogens, Vol. 5, pp. 1000354 (1-11), 2009.

[26] M. Sadr, A. Heidarinasab, H. Ahmad panahi and R. Safaeijavan, "Production and characterization of biocompatible nano-carrier based on Fe_3O_4 for magnetically hydroxychloroquine drug delivery," Polym. Adv. Technol. Vol. 32, pp. 564-573, 2021.

[27] D. Dozier, S. Palchoudhury and Y. Bao, "Synthesis of iron oxide nanoparticles with biological coatings," J. Environ. Sci. Health A, Vol. 7, pp. 16-18, 2010.

[28] A. OAU, "Prevention of Proteus mirabilis biofilm by surfactant solution," Egypt Acad. J. Biol. Sci, Vol.4, pp. 1-8, 2012.

[29] N.K. Pour, D.H. Dusane, P.K. Dhakephalkar, F.R. Zamin, S.S. Zinjarde and B.A. Chopade," Biofilm formation by Acinetobacter baumannii strains isolated from urinary tract infection and urinary catheters," FEMS Microbiol Immunol, Vol.62, pp. 328-338, 2011.

[30] S. Stepanović, D. Vuković and V. Hola, "Bonaventura GD, Djukić S, Ćirković I, Ruzicka F. Quantification of biofilm in microtiter plates: overview of testing conditions and practical recommendations for

assessment of biofilm production by staphylococci," Apmis, Vol.115, pp. 891-899, 2007.

[31] G. Unsoy, S. Yalcin, R. Khodadust, G. Gunduz and U. Gunduz," Synthesis optimization and characterization of chitosan-coated iron oxide nanoparticles produced for biomedical applications," J. Nanopart. Res. Vol. 14, pp. 964, 2012.

[32] M. Baniasadi, M. Tajabadi, M. Nourbakhsh and M. Kamali, "Synthesis and characterization of CORE-shell nanostructure containing super paramagnetic magnetite and poly (Amidoamine)(Pamam) dendrimers," 2014.

[33] Z. Hasanzadeh, G. Amoabedini, A. Seyfkordi and A. Vaziei, "Magnetic nanoparticles coated with starch environmental review was pragmatic compared to nanoparticles Magnetic," Biotech. News, Vol. 5, pp. 70-72, 2014.

[34] M.M. Mohammadi and A.A. Abdi, "Study of biofilm formation by pseudomonas aeruginosa using modified microtitre plate and scanning electron microscope," 2004.

[35] G. Nangmenyi, X. Li, S. Mehrabi, E. Mintz and J. Economy, "Silver-modified iron oxide nanoparticle impregnated fiberglass for disinfection of bacteria and viruses in water," Mater. Lett. Vol. 65, pp.1191-1193, 2011.

[36] T. Javanbakht, S. Laurent, D. Stanicki and K.J. Wilkinson, "Relating the surface properties of superparamagnetic iron oxide nanoparticles (SPIONs) to their bactericidal effect towards a biofilm of Streptococcus mutans," PLoS One, Vol. 11, pp. 0154445 (1-13), 2016.

[37] D.C. Kaur and S.V. Wankhede, "A study of Biofilm formation & Metallo-β-Lactamases in Pseudomonas aeruginosa in a tertiary care rural hospital," Int. j. sci. res. publ. Vol. 3, pp. (1-7) 2013.

[38] K. Smith and I.S. Hunter, "Efficacy of common hospital biocides with biofilms of multi-drug resistant clinical isolates, " J. Med. Microbiol. Vol. 57, pp. 966-973, 2008.

THIS PAGE IS INTENTIONALLY LEFT BLANK.